The ferric leaching kinetics of arsenopyrite

R. Ruitenberg [a,1], G.S. Hansford [b,*], M.A. Reuter [a,2],
A.W. Breed [b,3]

[a] *Raw Materials Technology Group, Faculty of Applied Earth Sciences, Delft University of Technology, Mijnbouwstraat 120, Delft, Netherlands*
[b] *Gold Fields Minerals Bioprocessing Laboratory, Department of Chemical Engineering, University of Cape Town, Rondebosch 7701, South Africa*

Abstract

In this investigation batch, ferric leaching experiments were carried out in a 100 mℓ jacketed vessel maintained at 25°C. The parameters varied during the course of the experimental program included the initial redox potential, the total iron concentration, the solids concentration and the pH of the leaching solution. The initial redox potential used ranged from 625 to 470 mV, the overall iron concentration ranged from 8 to 32 g.ℓ^{-1}, the mineral concentration ranged from 5 to 20 g.ℓ^{-1} and the initial pH used ranged from 1.10 to 1.45. The redox potential of the leach solution was monitored continuously using a redox probe connected to a computer. The leach rates were calculated from the measured change in the redox potential of the leaching solution. The variation in the ferric leaching rate of the arsenopyrite as a function of the solution redox potential displayed similar trends, irrespective of the conditions employed. The ferric leaching rate of the arsenopyrite decreased with decreasing redox potential of the leaching solution and could be accurately described using a modified Butler–Volmer equation; $-r_{Fe^{2+}} = r_0(e^{\alpha\beta(E-E')} - e^{(1-\alpha(\beta(E-E'))})$. High concentrations of ferric iron and protons, and a reduction in the solids concentration were found to impede the leach rate. The 'rest potential' (*i.e.*, the redox potential at which the dissolution of arsenopyrite stops) of the arsenopyrite was found to be higher under these conditions. However, no occluding sulphur layer could be detected on the surface of mineral particles, hence the results suggest that the reactivity of the mineral decreases with an increase in the effective concentration of the ferric iron species. Therefore, although the results suggest the

* Corresponding author. Fax: +21-21-6897579. E-mail: gsh@chemeng.uct.ac.za
[1] Present address: Bagijnhof 17, 2611 AN, Delft, The Netherlands. E-mail: rruitenberg@hotmail.com.
[2] Fax: +31-15-278-2836. E-mail: m.a.reuter@ta.tudelft.nl.
[3] Fax: +27-21-6897579. E-mail: ashli_breed@hotmail.com

likelihood of an electrochemical mechanism being operative, it is necessary to modify the Butler–Volmer-based model to account for the above observations in order to obtain a model capable of predicting the ferric leaching rate of arsenopyrite across a broad range of operating conditions. © 1999 Elsevier Science B.V. All rights reserved.

Keywords: Gold ores; Sulphide ores; Arsenopyrite; Leach kinetics; Extractive metallurgy

1. Introduction

Bioleaching is now an established technology for the pretreatment of refractory arsenical gold ores and concentrates. It offers economic, environmental and technical advantages over pressure oxidation and roasting [1,2]. Recent work on the bioleaching of pyrite has provided strong evidence that the bioleaching of sulphide minerals occurs via a two-step mechanism [3]. In this mechanism the mineral is leached chemically by ferric iron and the role of the bacteria is to regenerate ferric iron, thereby maintaining a high redox potential within the system. The existence of an indirect mechanism suggests that the bacterial and chemical subprocesses may be studied and optimised separately. Thus, there is a need for mechanistically based models that accurately describe the kinetics of these subprocesses. To date a number of models have been used to describe the ferric leaching kinetics of sulphide minerals [4–7]. The simplest model assumes a linear relationship between the redox potential of the solution and the mineral rest potential (E_{FeAsS}) [5]. Other postulated models include those based on electrochemical theory [4,7] and on the Monod equation [6].

If it is assumed that the bioleaching of arsenopyrite occurs via a similar mechanism, it is clear that the rate at which arsenopyrite is leached by ferric iron is an important step in the bioleaching of refractory arsenical gold ores and concentrates. However, although considerable work on the leaching of pyrite using ferric iron has been reported in the literature [7–10], to date very little work on the leaching of arsenopyrite, using ferric iron at concentrations and conditions similar to those used in bioleaching, has been reported. However, recent research has shown that the ferric leaching kinetics of pyrite [6,7] and arsenopyrite [11] may be dependent on the ferric–ferrous iron ratio (*i.e.*, redox potential), and not a function of the total or ferric iron concentrations.

Boon [6] suggested that the ferric leaching of pyrite could be described by means of Monod-type equation, Eq. (1);

$$v_{Fe^{2+}} = \frac{v_{Fe^{2+}}^{max}}{1 + B\dfrac{[Fe^{2+}]}{[Fe^{3+}]}} \tag{1}$$

However, May *et al.* [7] suggested that the ferric leaching of pyrite was an electrochemical (corrosion) phenomena, and hence chose to use an equation similar in form to the Butler–Volmer equation to describe the rate at which pyrite was leached by ferric iron, Eq. (2);

$$-r_{Fe^{2+}} = r_0\left(e^{\alpha\beta(E-E')} - e^{(1-\alpha)\beta(E-E')}\right) \tag{2}$$

According to the Butler–Volmer equation the dependence of the ferric leaching kinetics on the overpotential is linear at low overpotentials (0–20 mV). However, most bioleaching plants operate at higher overpotentials, which results in nonlinear kinetics.

To date studies on the ferric leaching rate of arsenopyrite have been complicated by controversy in the literature with regard to the stoichiometry of the leaching reaction. However, recent work has shown that the dissolution of arsenopyrite in ferric solution takes place according to Eq. (3) [11–13];

$$FeAsS + 5Fe^{3+} \rightarrow As^{3+} + 6Fe^{2+} + S^0 \tag{3}$$

The objective of this work was to determine whether or not the ferric leaching rate of arsenopyrite could be described using the modified form of the Butler–Volmer equation, Eq. (2), proposed by May et al. [7]. A further objective was to determine the effect of various parameters (i.e., $E_{initial}$, Fe_{total}, ρ_{solids}, and pH) on the ferric leaching kinetics of arsenopyrite.

2. Materials and methods

2.1. Experimental equipment

A diagrammatic representation of the experimental equipment is shown in Fig. 1. The experiments and the redox probe calibration were performed in a 100 mℓ jacketed glass vessel. The reactor had a H/D ratio of 1 and a working volume of 75 mℓ. The temperature in the reactor was maintained at 25°C by circulating water from a Grant Y6 constant temperature bath through the reactor jacket. Mixing was achieved by rotating a flat glass impeller via an overhead stirrer.
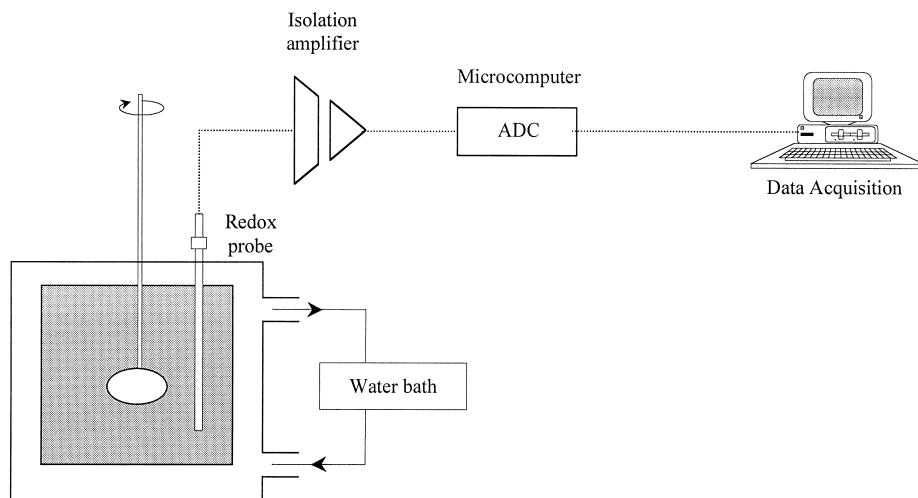

Fig. 1. Diagrammatic representation of the experimental equipment.

The redox potential of the leaching solution was measured using a Crison platinum wire–Ag/AgCl electrode filled with 3 M LiCl (198 mV vs. SHE). The redox electrode was connected via an optically isolated amplifier and an analogue to digital converter (ADC) on a single board microcomputer to a personal computer [14]. This allowed the redox potential of the leaching solution to be recorded continuously.

The parameters varied during the course of the experimental program included the initial redox potential, the total iron concentration, the solids concentration and the pH of the leaching solution. The initial redox potential used ranged from 625 to 470 mV, the overall iron concentration ranged from 8 to 32 g.ℓ^{-1}, the mineral concentration ranged from 5 to 20 g.ℓ^{-1} and the initial pH used ranged from 1.10 to 1.45.

2.2. Mineral used

The arsenopyrite used was obtained from Wards' (USA). Handpicked arsenopyrite crystals were ground using a pestle and mortar until the entire sample passed through a 100 μm sieve. Suspending the ground mineral in distilled water, allowing it to settle for a few minutes and then decanting the ultrafine material together with the liquid removed the ultrafines. The size analysis showed that 96.66% of the ground ore was finer than 106 μm, 63.27% was finer than 25 μm and 8.79% of the mineral was finer than 1 μm. The complete size analysis of the mineral is shown in Table 1. Analysis by laser diffraction with a Malvern Particle Sizer (UK) showed that the specific surface area of the ground material was 0.38 $m^2.g^{-1}$. The BET surface area was 1.97 $m^2.g^{-1}$.

The mineral was digested in HF [15] to determine the elemental composition of the arsenopyrite. It contained 25.4% As, 16.5% Fe, 0.5% Zn, 1% Pb and 19.7% sulphur. Scanning electron microscope (SEM) techniques confirmed the presence of these elements, and determined that the chief gangue mineral was quartz. The arsenopyrite content of the sample, estimated from the elemental analysis, was 48%.

2.3. Analyses

Distilled water and analytical grade laboratory chemicals were used for all the experimental work. The concentrations of ferrous and ferric iron in the leach solutions were determined by titration with potassium dichromate, $K_2Cr_3O_7$ [16]. Spent leach liquor was filtered through an 8 μm Millipore filter and the total iron and arsenic

Table 1
Size analysis of ground arsenopyrite mineral

Size fraction (μm)	Mass percent (%)
+106	3.34
−106+75	4.08
−75+53	9.95
−53+38	7.89
−38+25	11.5
−25	63.27

concentration determined by atomic adsorption spectroscopy. It was also titrated with cerium sulphate to determine the concentrations of ferrous iron, Fe^{2+}, and arsenite, As^{3+}.

2.4. Probe calibration

The total iron concentration, the counterions present, and the temperature of the solution affect the proportions of free ferric and ferrous iron in solution, hence the probe was calibrated at different total iron concentrations. However, the effect of arsenic was not considered. Ferrous and ferric sulphate solutions of similar concentrations were made up. An aliquot of ferric sulphate was added to the jacketed vessel, the redox probe inserted into the solution and the solution agitated. Once thermal equilibrium was achieved aliquots of ferrous sulphate were added, and the redox potential was recorded. The response of the logging system was rapid and the readings were found to be stable over long periods of time; e.g., a stable reading was achieved 2 s after a 30 mV step change in the solution redox potential.

The measured redox potential was plotted against $\log(Fe^{3+}/Fe^{2+})$, and the Nernst parameters, viz. RT/zF (slope) and E_0' (intercept), determined.

2.5. Experimental procedure

A ferric sulphate solution of the required concentration was made up and added to the jacketed vessel. The redox probe was inserted into the solution and the solution agitated. Once thermal equilibrium was achieved a known quantity of ore was added, and the redox potential monitored for the duration of the leach. The duration of the experiments was between 1 and 2 h.

2.6. Rate determination

The leaching rate was determined using the Nernst equation, the reaction stoichiometry of Eq. (3) and the measured variation in the redox potential of the slurry during the course of the experiment. Prior to performing the rate calculations it was necessary to smooth the raw data (E vs. t) in order to eliminate the scatter resulting from the differentiation of a noisy electronic signal. The general form of the smoothing equation found to give the best fit was;

$$E_{\text{fit}} = at^b + c \tag{4}$$

The constants a, b and c were found by minimising the sum of the squared errors. The values of E_{fit} were used to calculate dE/dt and the ferric–ferrous iron ratio as described below.

The ferric–ferrous iron ratio can be related to the solution redox potential, using the Nernst equation, viz.;

$$E = E_0' + \frac{RT}{zF} \ln\left(\frac{[Fe^{3+}]}{[Fe^{2+}]} \right) \tag{5}$$

In practice, and in this investigation, E_0' and RT/zF are determined by calibrating the redox probe at the conditions used.

Differentiating the Nernst equation (Eq. (5)) yields;

$$\frac{dE}{dt} = \frac{RT}{zF} \frac{d}{dt} \ln\left(\frac{[Fe^{3+}]}{[Fe^{2+}]}\right) \tag{6}$$

$$\frac{dE}{dt} = \frac{RT}{zF}\left(\frac{1}{[Fe^{3+}]}\frac{d[Fe^{3+}]}{dt} - \frac{1}{[Fe^{2+}]}\frac{d[Fe^{2+}]}{dt}\right) \tag{7}$$

The rate of arsenopyrite dissolution can be defined as;

$$r_{FeAsS} = \frac{d[FeAsS]}{dt} = -\frac{d[Fe_{total}]}{dt} = -\frac{d([Fe^{3+}] + [Fe^{2+}])}{dt} \tag{8}$$

Combining Eq. (7) with the reaction stoichiometry and Eq. (8) yields;

$$\frac{dE}{dt} = \frac{RT}{zF} r_{FeAsS}\left(\frac{5}{[Fe^{3+}]} + \frac{6}{[Fe^{2+}]}\right) \tag{9}$$

Rearranging Eq. (9) yields an expression for the rate of arsenopyrite leaching;

$$r_{FeAsS} = \frac{\dfrac{zF}{RT}\dfrac{dE}{dt}}{\dfrac{5}{[Fe^{3+}]} + \dfrac{6}{[Fe^{2+}]}} \tag{10}$$

The ferric ferrous ratio and the total iron concentration can then be used to determine the concentrations of both Fe^{3+} and Fe^{2+} using;

$$[Fe^{2+}] = \frac{[Fe_{total}]}{1 + \dfrac{[Fe^{3+}]}{[Fe^{2+}]}} \tag{11}$$

and

$$[Fe^{3+}] = \frac{[Fe_{total}]\dfrac{[Fe^{3+}]}{[Fe^{2+}]}}{1 + \dfrac{[Fe^{3+}]}{[Fe^{2+}]}} \tag{12}$$

Substituting Eqs. (11) and (12) into Eq. (10) yields an expression in which all the parameters can be determined. It is therefore possible to determine the variation in the

Table 2
Standard conditions for the ferric leaching of arsenopyrite

Parameter	Level
Volume (mℓ)	75
[Fe$_{total}$] (g.ℓ^{-1})	16
pH	1.1
Solids concentration (g.ℓ^{-1})	10
Agitator speed (rev.min^{-1})	1500
Temperature (°C)	25
$E_{initial}$ (vs. Ag/AgCl) (mV)	615

rate of arsenopyrite dissolution during the course of the experiment using the measured variation in the redox potential and the initial total iron concentration;

$$r_{FeAsS} = \frac{[Fe_{total}]\dfrac{zF}{RT}\dfrac{dE}{dt}}{\left(1 + \dfrac{[Fe^{3+}]}{[Fe^{2+}]}\right)\left(\dfrac{5}{\dfrac{[Fe^{3+}]}{[Fe^{2+}]}} + 6\right)} \tag{13}$$

Although the increase in the total iron concentration during the course of the experiments was small, $\pm 5\%$ of the initial iron concentration, it was taken into consideration during the calculation of the leaching rate.

The parameters varied during the course of the experimental program included the initial redox potential, the total iron concentration, the solids concentration and the pH of the solution. The standard ferric leaching conditions are shown in Table 2.

3. Results

3.1. Probe calibration

As the ferric leaching experiments were carried out under nonideal conditions it was necessary to determine the values of E_0' and RT/zF at the conditions used. The values of these parameters at 25°C and varying total iron concentrations are listed in Table 3.

Table 3
Comparison of theoretical and measured Nernst equation parameters ($T = 25$°C)

[Fe$_{total}$] (g.ℓ^{-1})	RT/zF (mV)	E_0 (mV)
8	25.78	430.9
16	27.21	430
32	28.38	431.9
Theoretical value	25.70	572

3.2. General behaviour

Although no attempt was made to confirm the reaction stoichiometry, upon completion of each experiment, the spent leach liquor was titrated with cerium sulphate and the presence of As^{3+} confirmed.

Fig. 2 shows the typical variation in the redox potential of the solution observed during the course of an experiment. From Fig. 2 it is apparent that during the first few minutes of leaching there is a rapid drop in the redox potential of the solution.

In all the experiments performed, raw data similar in shape to the data shown in Fig. 2 were obtained. After smoothing the raw data (Eq. (4)) the rate of ferrous iron production as a function of the redox potential of the leaching solution was determined (Eq. (13)) as described in Section 2.6.

3.2.1. Error analysis

The contribution of ferrous iron oxidation, by dissolved oxygen, to the ferric iron concentration, and hence the observed rate of ferric leaching was determined in an air-sparged CSTR. The feed to the reactor consisted of a salt solution containing 12 $g.\ell^{-1}$ ferrous iron. The temperature in the CSTR was maintained at 40°C; the residence time was maintained at 100 h and the pH was maintained at pH 1.75. Sparging compressed air at 100 $m\ell.min^{-1}$ through the solution ensured saturation of the liquid.

Fig. 3 shows the measured variation in the outlet ferrous iron concentration with elapsed time and the predicted variation in the outlet ferrous iron concentration if ideal CSTR behaviour, and no reaction, is assumed. The data in Fig. 3 were used to determine the approximate rate of ferric iron regeneration by oxidation of the ferrous iron. It was found to be in the region of 5.0×10^{-8} mol $Fe^{2+}.\ell^{-1}.s^{-1}$. In comparison, the ferrous iron production rates observed during the ferric leaching experiments ranged from about
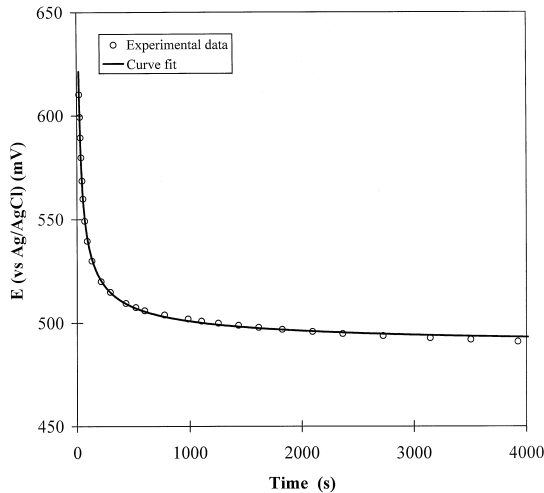

Fig. 2. Typical example of the observed variation in the redox potential with time, and curve fit ($y = 679.6\,x^{-0.56} + 486.6$; $R^2 = 0.998$) to experimental data.
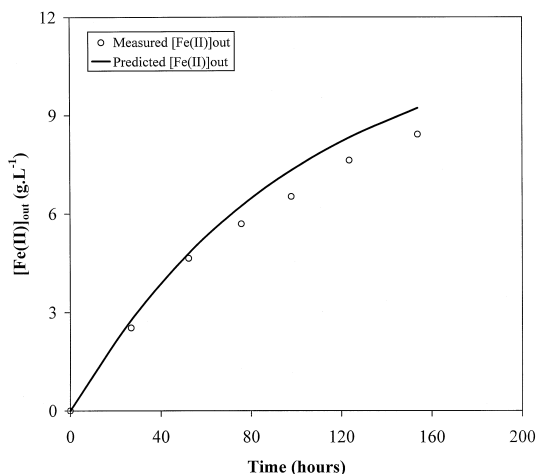
Fig. 3. Variation in the measured outlet ferrous iron concentration and the predicted variation in the outlet ferrous iron concentration if ideal CSTR behaviour and no reaction is assumed, with time.

5.5×10^{-6} mol $Fe^{2+}.\ell^{-1}.s^{-1}.(g \text{ FeAsS})^{-1}$ at the beginning of the experiment to about 2.7×10^{-8} mol $Fe^{2+}.\ell^{-1}.s^{-1}.(g \text{ FeAsS})^{-1}$ at the end of the experiment, i.e., from 8.9×10^{-5} to 4.3×10^{-7} mol $Fe^{2+}.\ell^{-1}.s^{-1}$, based on an arsenopyrite concentration of 16 g.ℓ^{-1}.

From the above it is clear that the rate of ferrous iron production during the leaching experiments could be ignored during the analysis of the kinetics of arsenopyrite leaching. For this reason no attempt was made to exclude oxygen from the leaching solution.

In addition to the above, analyses performed to determine the errors introduced as a result of attributing the drop in redox potential to the ferric leaching of arsenopyrite only were found to be in the region of 1%. The reproducibility was found to be in the region of 8%, hence it was possible to ignore the contributions of the ferric leaching of the copper, lead and zinc minerals in the sample to the changes in the redox potential of the solution. Furthermore, acid leaching tests performed in the absence of ferric iron were found to have little effect on the redox potential due to the low rates observed and the stoichiometry of the leaching reaction.

3.2.2. Leaching rate

Fig. 4 shows the specific rate of arsenopyrite leaching (expressed as the ferrous iron production rate per unit mass of arsenopyrite) as a function of the solution redox potential during one run. From Fig. 4 it is apparent that the rate initially increases with a decrease in the redox potential of the solution. It appears to pass through a maximum, and then decreases rapidly with a further decrease in the redox potential of the solution. However, it is clear that for most of the experiment, the rate of leaching decreased with a decrease in the redox potential of the solution.
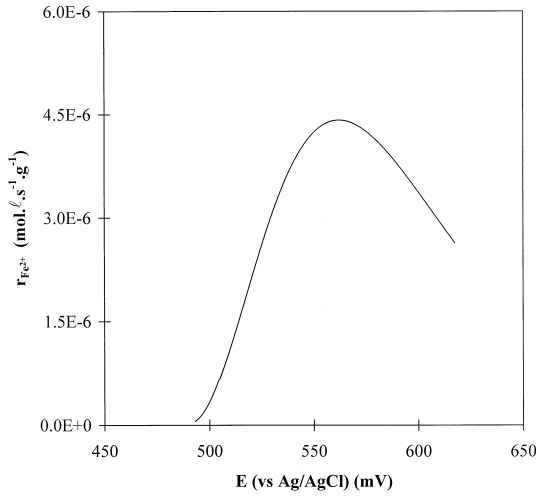
Fig. 4. Variation in the specific ferrous iron production rate during the ferric leaching of arsenopyrite as a function of the solution redox potential during one run.

3.3. Initial redox potential

The influence of the initial solution redox potential on the rate at which arsenopyrite is leached by ferric iron is shown in Fig. 5. From Fig. 5 it is clear that the initial increase in the leaching rate apparent in Fig. 4 is not visible at low initial redox potentials; viz.
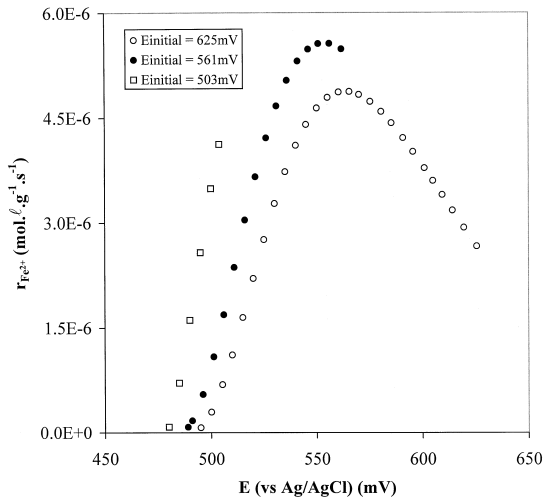

Fig. 5. Influence of the initial solution redox potential on the variation in the specific ferrous iron production rate during the ferric leaching of arsenopyrite, as a function of the solution redox potential.

$E_{initial} < 550$. Instead, the rate of leaching decreased with a decrease in the redox potential of the solution, across the entire range of redox potentials encountered.

3.4. Total iron concentration

The effect of the overall iron concentration on the ferric leaching kinetics of arsenopyrite was investigated at initial ferric iron concentrations of 8, 16 and 32 g.ℓ^{-1} (Fig. 6). From Fig. 6 it is apparent that an increase in the total iron concentration resulted in the ferric leaching reaction stopping at a higher value of the solution redox potential. It is also apparent that the maximum leaching rate observed at a total iron concentration of 8 g.ℓ^{-1} was significantly lower than at higher overall iron concentrations. Although this effect was reproducible, it was not supported by other findings.

3.5. Mass transfer

The results obtained during the experiments performed at different total iron concentrations suggest that, under the conditions employed, the rate of reaction is not mass-transfer limited. This was confirmed by experiments performed at impeller speeds ranging from 1250 to 1800 rev.min^{-1} and is consistent with the results of previous research performed at the same temperature [17].

3.6. Solids concentration

Fig. 7 shows the influence of the mineral concentration, at concentrations of 5, 10 and 20 g.ℓ^{-1}, on the ferric leaching of arsenopyrite. As in previous figures, the rate is expressed as the rate of ferrous iron production divided by the solids concentration. This
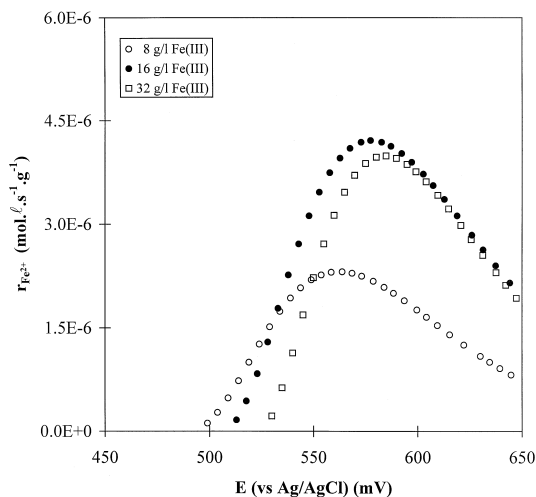

Fig. 6. Influence of the total iron concentration in solution on the variation in the specific ferrous iron production rate during the ferric leaching of arsenopyrite, as a function of the solution redox potential.
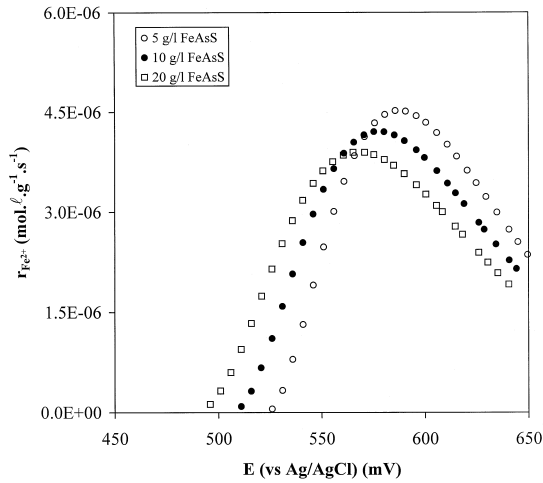
Fig. 7. Influence of the solids (arsenopyrite) concentration on the variation in the specific ferrous iron production rate during the ferric leaching of arsenopyrite, as a function of the redox potential of the solution.

was done in an attempt to eliminate the effect of the increase in the available surface area. From Fig. 7 it is clear that the rate based on the arsenopyrite surface area was not constant. However, the curves obtained show similar trends in the rate with changes in the solution redox potential.

The surface area concentration (arsenopyrite concentration) seems to affect the redox potential at which the leaching stops. It does not appear to have a significant influence on either the rate at which the leaching rate changed (the slope of the curve), or the maximum leaching rate of the arsenopyrite.

3.7. pH

Fig. 8 shows the influence of the solution pH upon the ferric leach rate of arsenopyrite. The mineral seems to be more active at lower acid concentrations.

3.8. Leached vs. unleached ore

Scanning electron microscopy (SEM) was used to determine whether or not the rate of leaching of the mineral used in this investigation was influenced by the formation of an occluding layer consisting of either jarosite or elemental sulphur. However, neither jarosite nor elemental sulphur was visible on the surface of a mineral sample that had been leached for 1 h. In addition, mineral that had been leached for 1 h was dried and leached once again, using fresh leaching solution. The results of the experiment performed using 'leached' arsenopyrite and the results of an experiment performed using unleached mineral, at the same conditions, are shown in Fig. 9. From Fig. 9 it is clear that the ferric leaching rate of 'leached' material is similar to the ferric leaching rate of fresh mineral.
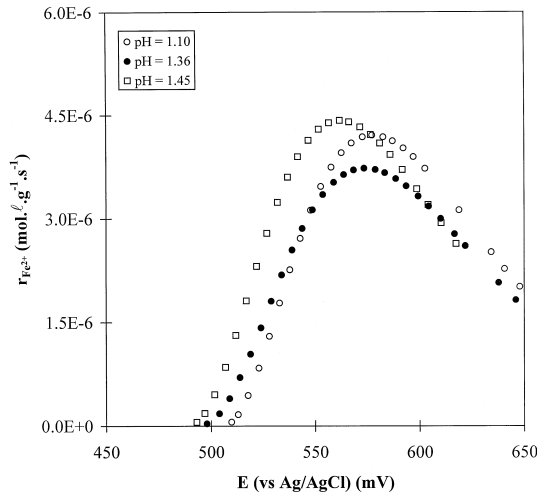
Fig. 8. Influence of the solution pH on the variation in the specific ferrous iron production rate during the ferric leaching of arsenopyrite, as a function of the redox potential of the solution.

3.9. Kinetics

It is apparent from Figs. 4–9 that the relationship between the redox potential of the solution and the specific rate of ferrous iron production is not linear. It was not possible to fit the electrochemically-based model proposed by Verbaan and Crundwell [4], or the Monod-type model proposed by Boon [6]. However, it was possible to model the ferric leach kinetics using the Butler–Volmer-based model suggested by May et al. [7]
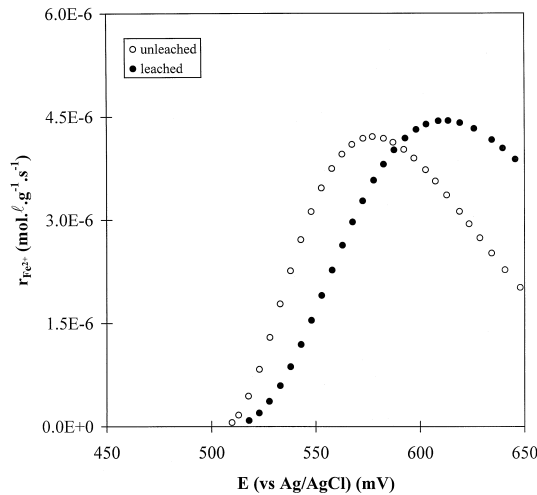

Fig. 9. Comparison between the variation in the specific ferrous iron production rate during the ferric leaching of unleached and leached arsenopyrite, as a function of the redox potential of the solution.
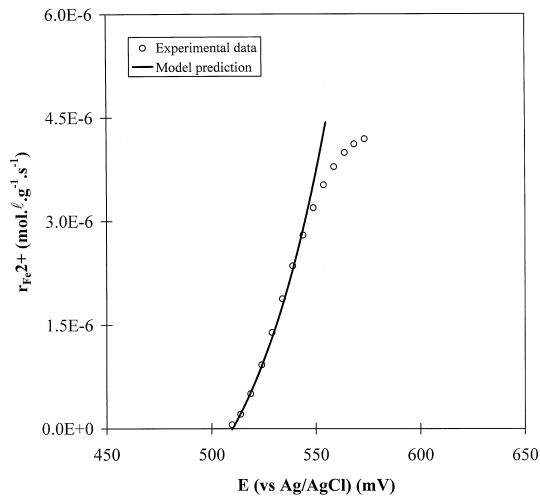
Fig. 10. Comparison between the Butler–Volmer based model prediction ($r_0 = 5 \times 10^4$, $\alpha = 0.498$, $\beta = 0.0272$, $E' = 510$) and the experimental leaching rate data.

(Eq. (2)). Comparison of the Butler–Volmer-based model prediction with a typical set of experimental results is shown in Fig. 10. It is clear from Fig. 10 that the agreement between the model based on the Butler–Volmer equation and the experimental results is good.

4. Discussion

The rapid change in the initial redox potential shown in Fig. 2 was anticipated, and can be explained as follows. At high total iron concentrations and ferric–ferrous ratios, even a small increase in the ferrous iron concentration will result in a large change in the ferric ferrous ratio, and hence a large drop in the redox potential.

In most of the experiments performed the ferric leaching rate of arsenopyrite initially increased with a decrease in the redox potential of the solution (Figs. 4–8). The leaching rate reached a maximum, and then decreased rapidly with a further decrease in the redox potential.

An increase in the initial ferric leaching rate with decreasing redox potential was also observed during the ferric leaching of pyrite [7]. However, although a drop in the ferric leaching rate of arsenopyrite was observed at redox potentials between 600 and 700 mV (vs. SHE) [18], the behaviour apparent in Figs. 4–8 has not been reported previously for arsenopyrite. It is therefore suggested that this *transient* behaviour is a result of the rearrangement of the ions on the surface of the mineral and in the electrical double layer surrounding the mineral; it is not a result of the leaching of the mineral itself. This postulate is supported by observations made during studies on the effect of the ferric iron concentration on the eletrophoretic mobility of arsenopyrite [19], and by the fact that no surface products responsible for passivation of the mineral surface were observed.

Although previous workers have detected a sulphur layer on the mineral surface after both the acid, and the ferric leaching of arsenopyrite, it has not been found to hinder the dissolution reaction [12,18,20,21]. The absence of a surface layer in this investigation may be a result of the high redox potentials used [22]. Furthermore, the reactive nature of the leached mineral suggests that the rate of leaching is not time-dependent and is primarily a function of the redox potential of the leaching solution. The slight increase in the rate of dissolution of the 'leached' mineral can be attributed to the increase in the surface area.

The decrease in the rate of leaching with a decrease in the redox potential of the solution observed for most of the experiment is in agreement with previously reported trends for the ferric leaching of sulphide minerals [7,11,23–25]. This suggests a dependency of the ferric leaching rate on the redox potential of the leaching solution, which in turn suggests that an electrochemical model be used to describe the ferric leaching kinetics of arsenopyrite.

An electrochemically driven reaction should exhibit a half-order dependence on the ferric iron concentration [26]. However, the ferric leaching rate of pyrite was found to be independent of the total iron concentration, for iron concentrations ranging from 0.05 to 0.5 M (2.80 to 28 g.ℓ^{-1}) [7]. Although the leaching rate of arsenopyrite did not exhibit a half-order dependence on the ferric iron concentration it was not found to be independent of the total iron concentration (Fig. 6). In addition, it was not possible to fit the models proposed by either Verbaan and Crundwell [4] or Boon [6].

It was possible to model the ferric leach kinetics of arsenopyrite across a wide range of conditions using the Butler–Volmer based model suggested by May et al. [7] (Eq. (2)). However, a limitation of the model appears to be its dependence on the 'rest potential' of the mineral, i.e., the redox potential of the solution at which at which the dissolution of arsenopyrite stops. This arsenopyrite 'rest potential' was found to increase when:

(i) the starting potential increases,
(ii) the total iron concentration increases,
(iii) the solids concentration decreases, and
(iv) the H^+ concentration increases.

Although pH has been reported to have an effect on the rest potential of molybdenite [23], it is more likely that the effect of pH on the rate of leaching can be attributed to its effect on the speciation of the ferric sulphate complexes. pH has a significant effect on the complexes formed between Fe^{3+} and SO_4^{2-} over the range from pH 1.0 to 2.0 [27]. The different complexes would in turn be expected to have different leaching capabilities.

The results therefore suggest that the reactivity of the mineral is determined by the ferric and proton concentration based on the arsenopyrite surface area. An increase in the concentration of either ferric iron or protons (relative to the arsenopyrite surface area) results in a reduction in the reactivity of the mineral. This is regarded as highly unusual as most reaction mechanisms are favoured by an increase in reactant concentration.

Although the underlying mechanism responsible for the observed influence of the different parameters on the leaching rate is not clear at present, it is suspected that they

affect the speciation of the iron, sulphur and arsenic complexes in the solution. It is therefore necessary to modify the Butler–Volmer-based model to include the effect of parameters such as the pH and the ferric iron concentration on the activity of the ferric and ferrous iron species involved. This may yield a mechanistically based model capable of predicting the ferric leaching rate of minerals over a wide range of conditions.

Acknowledgements

Appendix A

a	constant in smoothing equation (s^{-1})
B	kinetic constant (dimensionless)
b	constant in smoothing equation (dimensionless)
c	constant in smoothing equation (dimensionless)
E	solution redox potential (mV)
E'	mineral rest potential (mV)
E'_0	constant in Nernst equation (mV)
F	Faraday constant $(C.mol^{-1})$
$[Fe^{2+}]$	ferrous iron concentration $(mol.\ell^{-1})$
$[Fe^{3+}]$	ferric iron concentration $(mol.\ell^{-1})$
$[Fe_{total}]$	total iron concentration $(mol.\ell^{-1})$
R	universal gas constant $(kJ.K^{-1}.mol^{-1})$
r_0	kinetic constant in chemical ferric mineral oxidation $(mol.\ell^{-1}.h^{-1})$
$r_{Fe^{2+}}$	arsenopyrite leaching rate $(mol.\ell.s^{-1}.g^{-1})$
r_{FeAsS}	arsenopyrite leaching rate $(mol.\ell.s^{-1}.g^{-1})$
T	absolute temperature (K)
t	time (s)
z	number of electrons involved in a reaction (dimensionless)
α	fraction of mineral reacted at time, t (dimensionless)
β	zF/RT (dimensionless)
$v_{Fe^{2+}}^{max}$	maximum area specific ferrous iron production rate $(mol.m^{-2}.h^{-1})$
$v_{Fe^{2+}}$	area specific ferrous iron production rate $(mol.m^{-2}.h^{-1})$

References

[1] P.C. Van Aswegen, Commissioning and operation of bio-oxidation plants for the treatment of refractory gold ores, in: J.B. Hiskey, G.W. Warren (Eds.), Hydrometallurgy; Fundamentals, Technology and Innovations, Soc. Min. Metall. Explor. AIME, 1993. pp. 709–725.
[2] R. Poulin, R.W. Lawrence, Economic and environmental niches of biohydrometallurgy, Minererals Engineering 9 (8) (1996) 799–810.

[3] M. Boon, G.S. Hansford, J.J., Heijnen, The role of bacterial ferrous iron oxidation in the bioleaching of pyrite, in: T. Vargas, C.A. Jerez, J.V. Wiertz, H. Toledo (Eds.), Biohydrometallurgical Processing Vol. I, University of Chile, Santiago, 1996, pp. 153–163.

[4] B. Verbaan, F.K. Crundwell, An electrochemical model for the leaching of a sphalerite concentrate, Hydrometallurgy 16 (3) (1986) 345–359.

[5] S. Nagpal, D. Dahlstrom, T. Oolman, A mathematical model for the bacterial oxidation of a sulfide ore concentrate, Biotechnology and Bioengineering 43 (5) (1994) 357–364.

[6] M. Boon, 1996. Theoretical and experimental methods in the modelling of bio-oxidation kinetics of sulphide minerals, Ph.D thesis, Delft University of Technology, The Netherlands.

[7] N. May, D.E. Ralph, G.S. Hansford, Dynamic redox potential measurements for determining the ferric leach kinetics of pyrite, Minerals Engineering 10 (11) (1997) 1279–1290.

[8] R.M. Garrels, M.E. Thompson, Oxidation of pyrite by iron sulphate solutions, American Journal of Science 258A (1960) 57–67.

[9] C.T. Mathews, R.G. Robins, The oxidation of iron disulphide by ferric sulphate, Australian Chemical Engineering (August 1972) 21–25.

[10] M.A. McKibben, H.B. Barnes, Oxidation of pyrite in low temperature acidic solutions: Rate laws and surface textures, Geochimica et Cosmochimica Acta 50 (7) (1986) 1509–1520.

[11] A.W. Breed, S.T.L. Harrison, G.S. Hansford, A preliminary investigation of the ferric leaching of a pyrite/arsenopyrite flotation concentrate, Minerals Engineering 10 (9) (1997) 1023–1030.

[12] N. Iglesias, I. Palencia, F. Carranza, Removal of the refractoriness of a gold bearing pyrite–arsenopyrite ore by ferric sulphate leaching at low concentration, in: J.P. Hager (Ed.), EPD Congress 1993, The Minerals, Metals and Materials Society, 1993, pp. 99–115.

[13] J. Zeman, M. Mandl, P. Mrnustíková, Oxidation of arsenopyrite by *Thiobacillus ferrooxidans* detected by a mineral electrode, Biotechnology Techniques 9 (2) (1995) 111–116.

[14] E.W. Randall, P. Moon, A.D.M. Gavin, Dynamically extendable communications protocol for a serial input/output system, Journal of Microcomputer Applications 16 (1993) 385–393.

[15] A.D. Bailey, An assessment of oxygen availability, iron build-up and the relative significance of free and attached bacteria, as factors affecting bio-oxidation of refractory gold-bearing sulphides at high solids concentrations, PhD thesis, University of Cape Town, South Africa, 1993.

[16] G.H. Jeffrey, J. Bassett, J. Mendham, R.C. Denney, Vogel's Textbook of quantitative chemical analysis, 5th edn., Longman, New York, 1989.

[17] N. Iglesias, I. Palencia, F. Carranza, Treatment of a gold bearing arsenopyrite concentrate by ferric sulphate leaching, Minerals Engineering 9 (3) (1996) 317–330.

[18] J.G. Dunn, P.G. Fernandez, H.C. Hughes, H.G. Linge, Aqueous oxidation of arsenopyrite in acid, Final Proc. Austral. Inst. Min. Metall. Annual Conference, Australasian Institute of Mining and Metallurgy, Carlton, Australia, 1989, pp. 217–220.

[19] A. MacDonald, G.S. Hansford, Zeta potential measurement of Thiobacillus ferrooxidans and Leptospirillum ferrooxidans in the presence of pyrite, Biotech SA '97, Rhodes University, Grahamstown, South Africa, 1997, p. 57.

[20] G.M. Kostina, A.S. Chernyak, Electrochemical conditions for the oxidation of pyrite and arsenopyrite in alkaline and acid solutions, Zhurnal Prikladnoi Khimii 49 (7) (1976) 1534–1570.

[21] I. Lázaro, R. Cruz, I. González, M. Monroy, Electrochemical oxidation of arsenopyrite in acidic media, International Journal of Minerals Processing 50 (1–2) (1997) 63–75.

[22] H. Tributsch, Personal communication, 1997.

[23] P.F. Jorge, G.P. Martins, Electrochemical and other aspects of indirect electrooxidation process for the leaching of molybdenite by hyperchloride, in: R.G. Bautista, R.J. Wesely, G.W. Warren (Eds.), Hydrometallurgical Reactor Design and Kinetics, The Metallurgical Society, 1986, pp. 263–292.

[24] F.K. Crundwell, Kinetics and mechanism of the oxidative dissolution of a zinc sulphide concentrate in ferric sulphate solutions, Hydrometallurgy, 19 (2) 227–242.

[25] B. Verbaan, R. Huberts, An electrochemical study of the bacterial leaching of synthetic nickel sulfide (Ni_3S_2), International Journal of Mineral Processing 24 (3–4) (1988) 185–202.

[26] D. Pletcher, Industrial Electrochemistry, Chapman & Hall, New York, 1984.

[27] J. Barrett, M.N. Hughes, G.I. Karavaiko, P.A. Spencer, Metal extraction by bacterial oxidation of minerals, Ellis Horwood, New York, 1993.